Protist, Vol. 171, 125710, February 2020
http://www.elsevier.de/protis
Published online date 7 December 2019

Protist

ORIGINAL PAPER

Molecular Phylogeny of Marine Gregarines (Apicomplexa) from the Sea of Japan and the Northwest Pacific Including the Description of Three Novel Species of *Selenidium* and *Trollidium akkeshiense* n. gen. n. sp.

Kevin C. Wakeman[1]

Institute for the Advancement of Higher Education, Hokkaido University, 060-0810 Japan

Submitted May 24, 2019; Accepted December 1, 2019
Monitoring Editor: Frank Seeber

This study set out to bolster morphological and molecular datasets of marine gregarine apicomplexans. Gregarines were sampled from the Sea of Japan and Northwest Pacific from cirratuliform polychaetes (Acrocirridae, Cirratulidae, and Flabelligeridae), as well as sipunculids. Trophozoites (feeding stages) were gathered for identification using light microscopy, scanning electron microscopy, and transmission electron microscopy. Cells were also collected for molecular phylogenetic analysis using 18S rDNA and 28S rDNA. As a result, three new species of *Selenidium*, *S. planusae* n. sp., *S. validusae* n. sp., and *S. pyroidea* n. sp. were described, and additional morphological and genetic data were gathered for an existing species, *S. orientale*; and *Trollidium* was established as a new genus. *Trollidium akkeshiense* n. gen. n. sp. possessed a unique, unsymmetrical organization of microtubules running the longitudinal length of one side of the trophozoite, corresponding to a zig-zag pattern of epicytic (surface) folds, and a flicking pattern of movement. Phylogenetic analyses of 18S rDNA and 28S rDNA showed that these portions of the ribosomal operon are able to resolve some relationships among *Selenidium*, while other lineages including *Trollidium akkeshiense* n. gen. n. sp. appeared to be highly influenced by long branch attraction. High evolutionary rates along the ribosomal operon of gregarines may hinder this marker from resolving deeper nodes among early apicomplexans.

Key words: Archigregarines; evolutionary morphology; marine parasites; systematics; ultrastructure.

Introduction

Gregarines represent the most diverse group of apicomplexans. These parasites are found in invertebrates, typically infecting the gut and coelomic cavities of their hosts. Those gregarine apicomplexans from marine hosts (marine gregarines), have been traditionally lumped into two groups: archigregarines and eugregarines (Adl et al. 2019; Grassé 1953; Levine 1971, 1976, 1977a, b). Archigregarines have maintained many pleisiomorphic

[1]fax +81 11 706 4851.
e-mail wakeman.k@oia.hokudai.ac.jp

https://doi.org/10.1016/j.protis.2019.125710

traits such as myzocytosis, feeding using a distinct apical complex, trophozoite stages with morphological and behavior traits similar to that of the infective stages (sporozoites) of other apicomplexans, and exclusively infecting the intestines of a single marine host (Schrével 1971a; Schrével et al. 2016). Eugregarines are inferred to be more derived, having features such as gliding motility using a relatively rigid cytoskeleton consisting of many (hundreds) of epicytic folds on the cell surface, and can be found across not only marine hosts, but those in freshwater, and terrestrial environments as well (Desportes and Schrével 2013a, b). Together, these gregarine apicomplexan lineages are key to understanding the early evolution and diversification of apicomplexans as a whole (Cox 1994; Leander 2008; Théodoridès 1984). Still, gregarine apicomplexans, especially marine gregarines, are notably understudied; and owing to a lack of molecular data, classification schemes, and the relationship of gregarines to other apicomplexan groups, remain ambiguous (Rueckert and Horák 2017; Wakeman and Leander 2012).

Among the ancestral lineages of marine gregarines, the majority have been classified into the genus *Selenidium* Giard, 1884. This genus is generally defined by the presence of relatively few surface folds that are subtended by a layer of microtubules on an elongated trophozoite stage that bends and twists in a nematode-like fashion (Desportes and Schrével 2013a, b). The systematics and classification of *Selenidium* in currently uncertain and has been a topic under consideration for some time (Levin 1971), although these proposed schemes are themselves not well supported in light of molecular datasets (Paskerova et al. 2018; Schrével et al. 2016). The primary issue is likely due to the fact that the defining characteristics of *Selenidium* are shared among other pleisiomorphic gregarine lineages, and even other basal marine alveolates, resulting in polyphyletic groupings. Such is the case with *Platyproteum vivax* (Ex. *Selenidium vivax* Gunderson and Small, 1986), a parasite of sipunculids that was initially classified as a member of the *Selenidium* based on its movement and general ultrastructure (Gunderson and Small 1986). However, molecular data later supported the establishment of a novel genus, *Platyproteum* (Rueckert and Leander 2009); it has been further suggested that *Platyproteum* is a stem group, being more closely related to dinoflagellates (and other alveolates) than to apicomplexans (Cavalier-Smith 2014).

To date, 26 18S rDNA sequences and only two 28S rDNA sequences have been generated from *Selenidium*. In the SSU datasets these sequences span four clades, which correspond to the host groups from which *Selenidium* have been isolated: terebellids, sipunculids, cirratulids, as well as another clade consisting of mostly tube-forming polychaetes (containing the type species, *S. pendula*, Giard 1884) (Rueckert and Horák 2017; Schrével et al. 2016). The relationships between these clades has yet to be resolved. Therefore, it is unclear whether *Selenidium* is a true group or represents cases of convergent or parallel evolution. While 28S rDNA datasets do show some promise in resolving some of this evolutionary history, there is still a lack of data for this particular marker, and so more data is needed to evaluate its suitability for resolving the phylogeny of gregarine apicomplexans (Paskerova et al. 2018).

In the present study, four marine gregarine species within the genus *Selenidium*, and a novel lineage, *Trollidium akkeshiense* n. gen. n. sp., were isolated from a sipunculid, as well as cirratuliform polychaetes (Acrocirridae, Cirratulidae, and Flabelligeridae). The morphology and ultrastructure of these parasites was studied using light microscopy and electron microscopy. Molecular data from 18S rDNA as well as 28S rDNA were amplified with the goal of placing *Selenidium* and gregarines in a more robust phylogenetic framework.

Results

Morphological Observations

Trophozoites of *Selenidium planusae* n. sp. were isolated from *Cirriformia tentaculata* Montagu, 1808 and had an average length of 124 μm (115–137 μm, $n = 32$), width of 27 μm (22–35, $n = 32$), and thickness of 5 μm ($n = 3$). These cells had a translucent appearance and were elongate with a central nucleus that was ovoid or spherical (average length = 10 μm, $n = 30$; average width 7 μm, $n = 30$). Cells moved by bending. The mucron narrowed to a point (Fig. 1A, B, E; Supplementary Material Table S1). Syzygy was caudo-frontal (Fig. 1C). Cells were compressed in cross-section, with an average thickness of 10 μm (Fig. 1D). Under a scanning electron microscope, the surface appeared to have shallow folds (Fig. 1D–F). Thin cross-sections of *S. planusae* n. sp. trophozoites did not reveal obvious epicytic folds (Fig. 2A). Sections through the mucron revealed rhoptries and microtubules (Fig. 2B, C). Cells were filled with amylopectin granules as well as intracisternal gran-

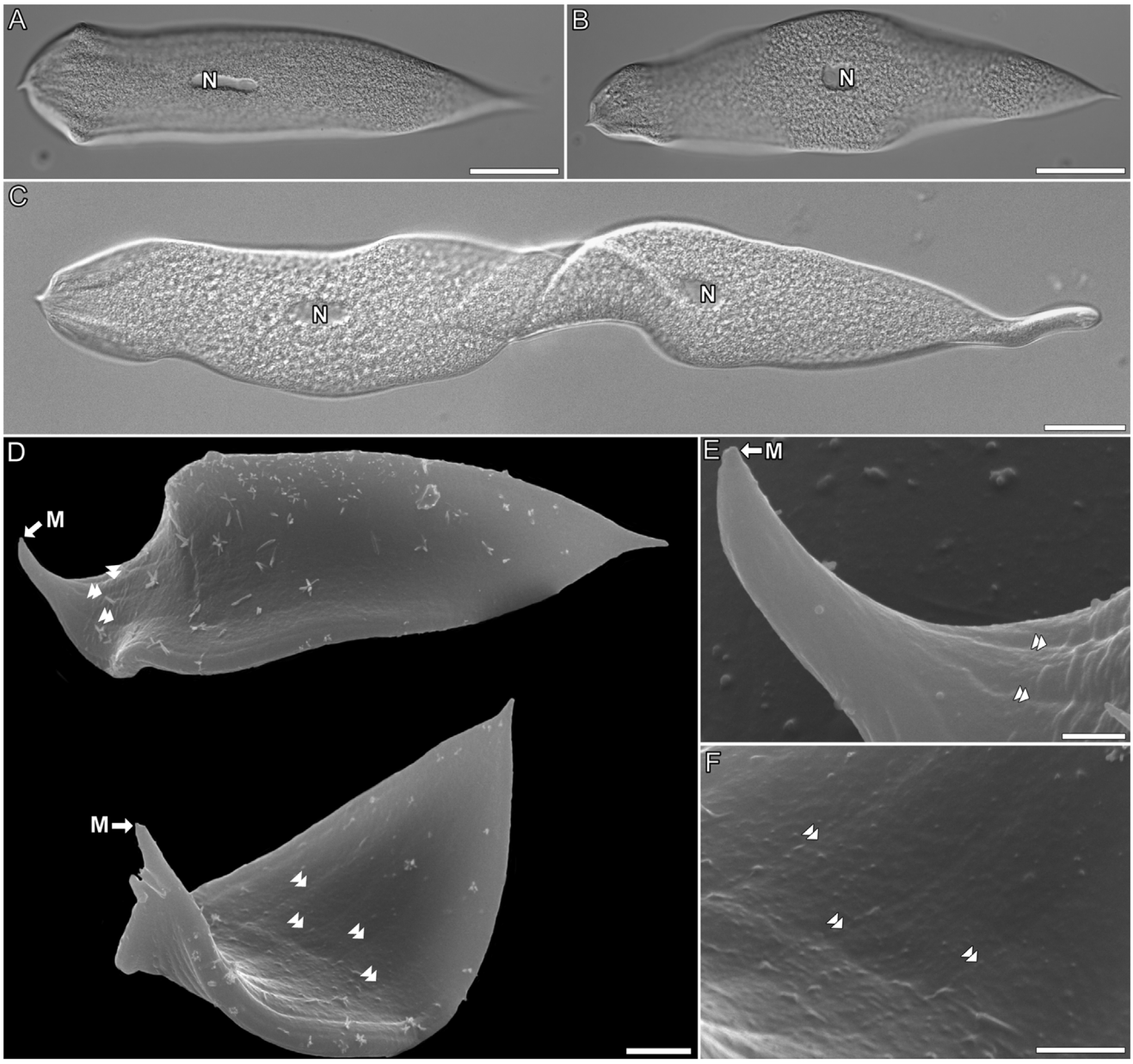

Figure 1. Light micrographs and scanning electron micrographs showing the general morphology of *Selenidium planusae* n. sp. **A, B.** Trophozoites with mucrons (oriented left) with a central nucleus (N). **C.** Gamonts in syzygy (caudo-frontal). **D.** Scanning electron micrographs of trophozoites showing the pointed mucron (M). Some shallow folds (double arrowheads) appear to be visible on the surface. **E.** High-magnification images of the pointed mucron (M) and shallow anterior folds (double arrowheads). **F.** High-magnification images of the shallow folds (double arrowheads) centrally located on the trophozoite. Scales: A–C = 10 μm; D = 5 μm; E, F = 1 μm.

ules (Figs 2A, 3A–C). Microtubules subtending the trilayer membrane were also observed (Fig. 3C).

Trophozoites of *Selenidium validusae* n. sp. were isolated from *Acrocirrus validus* Marenzeller, 1979 and were compressed and elongate with an average length of 178 μm (152–202 μm, $n = 30$), width of 21 μm (18–25 μm, $n = 30$) (Fig. 4A, B), and thickness of 8 μm ($n = 4$). The nucleus was generally ovoid with a prominent nucleolus, having an average length of 13 μm (11–14 μm, $n = 15$) and

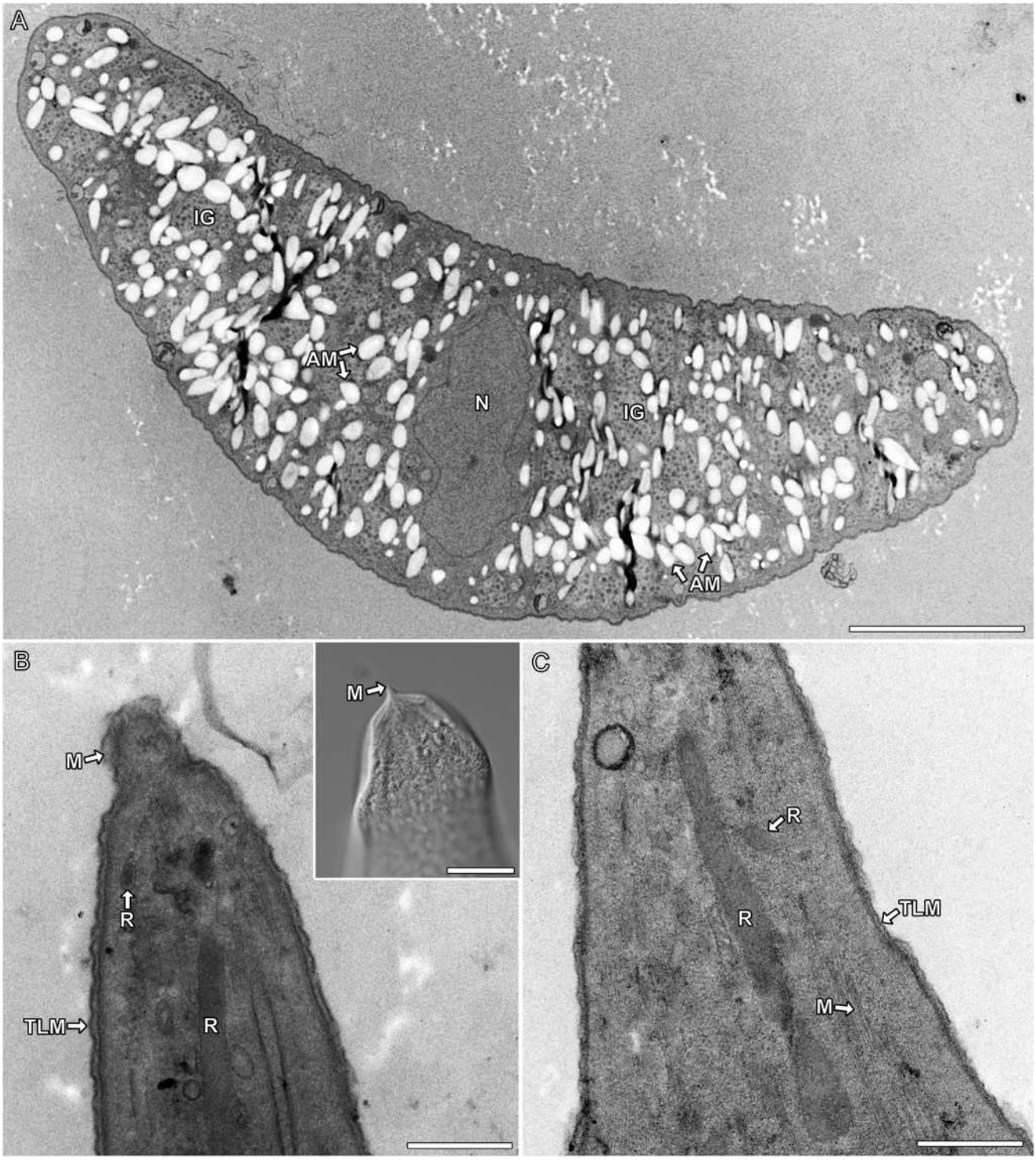

Figure 2. Transmission electron micrographs of *Selenidium planusae* n. sp. **A.** Cross-section through a trophozoite showing the nucleus (N), amylopectin granules (AM), and intracisternal granules (IG). **B–C.** High-magnification longitudinal-sections through the anterior part of the trophozoite and mucron (M) showing the trilayer membrane (TLM), and rhoptries (R) and microtubules (M); the corresponding region of the cell is shown in the inset. Scales: A = 5 μm; B = 2 μm; B (inset) = 10 μm; C = 1 μm.

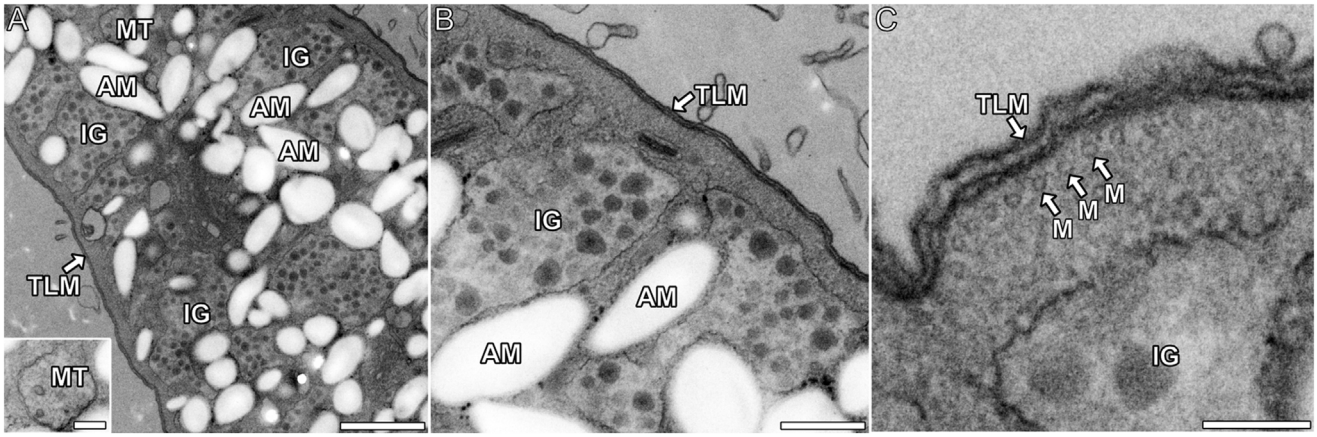

Figure 3. Transmission electron micrographs of *Selenidium planusae* n. sp. **A, B.** Cross-sections showing the trilayer membrane (TLM), amylopectin granules (AM), a mitochondrion (MT, inset), and intracisternal granules (IG).**C.** Cross-section showing the layers of the trilayer membrane (TLM), microtubules (M) subtending the membrane of the cell, as well as a sack of viral particles (V) showing capsids (C).Scales: A = 1 μm; A (inset) = 100 nm; B = 500 nm; C = 100 nm.

width of 10 μm (9–12 μm, $n = 15$). Cells moved by bending. Syzygy was observed to be caudal (Fig. 4B inset). The mucron of *S. validusae* n. sp. narrowed to a point; refractile bodies, interpreted to be rhoptries were visible in this region (Fig. 4A, C, D). Thin sections viewed under a transmission electron microscope showed microtubules subtending the trilayer membrane (Fig. 5A). Amylopectin granules as well as intracisternal granules were visible (Figs 5A, B, 6A). Also abundant were putative organelles of unknown origin. These were ovoid, measuring on average 175 nm × 300 nm ($n = 50$), and possessed thread-like (reminiscent of thylakoids) spindles spanning the width of the organelle (Fig. 6 A–C).

Trophozoites of *Selenidium pyroidea* n. sp. were isolated from *Themiste pyroides* Chamberlin, 1919 and were elongate with an average length of 309 μm (252–402 μm, $n = 20$) and width of 35 μm (24–43 μm, $n = 20$). The centrally-located nucleus was ovoid, with an average length of 9 μm (7–12 μm, $n = 17$) and width of 30 μm (22–37 μm, $n = 17$) (Fig. 7A, B). Cells moved by slowly bending and were brown in appearance. The surface of the cell was covered with 37 epicytic folds (Figs 7C, E, 8A) that extended up to the rounded mucron (Fig. 7D). Thin sections of *S. pyroidea* n. sp. revealed an accumulation of lipids and amylopectin (Fig. 8A, B). Mitochondria and microtubules were observed beneath the trilayer membrane (Fig. 8C–D). Numerous Golgi apparatus were observed throughout the cytoplasm (Fig. 8F, G).

Trophozoites of *Selenidium orientale*, also from *Themiste pyroides*, were elongate with an average length of 273 μm (252–345 μm, $n = 15$) and width of 15 μm (11–32 μm, $n = 15$). The centrally-located nucleus was ovoid, with an average length of 7 μm (5–11 μm, $n = 13$) and width of 12 μm (9–15 μm, $n = 13$) (Fig. 9A, B). Cells were more or less translucent. The surface of the cell was covered with 17 epicytic folds that extended from just below the mucron (Fig. 9C–E). Thin cross-sections through *S. orientale* showed that the cells were filled with amylopectin granules, and some lipids (Fig. 10A). The epicytic folds were bulbous, being slightly compressed just below the tip, and wider at the base (Fig. 10A, B). The folds consisted of mitochondria and layers of microtubules below the trilayer membrane (Fig. 10B).

Trophozoites of *Trollidium akkeshiense* n. gen. n. sp. isolated from *Pherusa plumose* Müller, 1776 were elongate with an average length of 218 μm (201–243 μm, $n = 20$) and width of 20 μm (17–24 μm, $n = 20$). The centrally-located nucleus was ovoid, with an average length of 17 μm (14–18 μm, $n = 15$) and width of 10 μm (9–12 μm, $n = 15$) (Fig. 11A, B). In the light micrograph images of the trophozoites, the surface appeared to wrinkle slightly (Fig. 11B). Video recordings made of *T. akkeshiense* n. gen. n. sp. showed that the cell had a single direction that the cell would constrict and subsequently thrash/flick; this region corresponded to the unique fold pattern on the trophozoites surface (Supplemental Video 1). The cell was covered in 103 epicytic folds that ran from the mucron to

Figure 4. Light micrographs and scanning electron micrographs showing the general morphology of *Selenidium validusae* n. sp. **A, B.** Light micrographs showing the general morphology of trophozoites. The nucleus (N) is centrally located, and rhoptries (arrows) are visible as refractile bodies in the images. Mucrons have been oriented towards the top. **B (inset).** Pair of gamonts in caudal syzygy (asterisk); the mucron (M) is oriented toward the bottom. **C.** High-magnification light micrograph of the mucron showing refractive rhoptries (arrows). **D.** Scanning electron micrographs showing the general morphology of trophozoites; mucrons are oriented to the right. Scales: A, B = 10 μm; B (inset) 20 μm; C = 1 μm; = 15 μm; D = 5 μm.

the posterior end of the cell (Fig. 11C; Fig. 12A). On one side of the trophozoites, the folds appeared to zig-zag (Fig. 11D, F). The mucron and posterior ends were rounded, and the mucron had a disc-like protrusion (Fig. 11E). Thin sections through the trophozoites of *T. akkeshiense* n. gen. n. sp. showed that the network of longitudinal microtubules ran down only one side of the cell (Fig. 12A) – the side adorned with the zig-zag pattern of epicytic folds (Fig. 12D); amylopectin granules, lipids, mitochondria, and Golgi apparatus were also observed (Fig. 12A–D).

Molecular Analyses

In the analysis of the 18S rDNA, the novel sequences generated from *Selenidium* in this study were split between three well-supported clades; *S. validusae* n. sp. branched together with *S.* cf. *echinatum* within a clade containing the type species of *Selenidium*, *S. pendula* (Fig. 13). Some of the nodes within this particular clade garnered low to moderate statistical support in the Maximum Likelihood and Bayesian analyses. *Selenidium pyroidea* n. sp. and *S. orientale* (Japan) branched in a clade

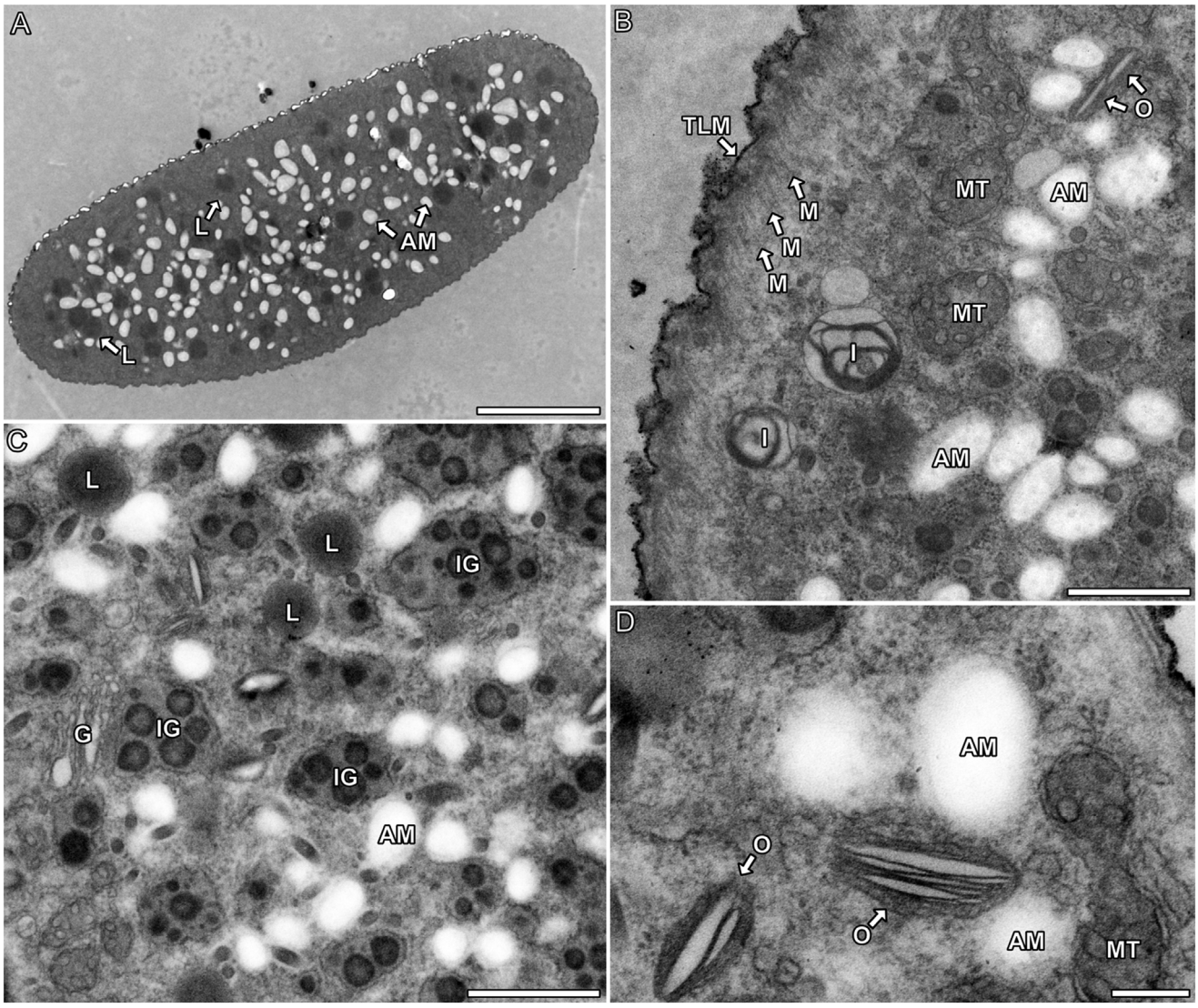

Figure 5. Transmission electron micrographs of *Selenidium validusae* n. sp. **A.** Cross-section through a trophozoite showing the outline of the cell containing amylopectin granules (AM) and lipids (L). **B.** Tangential section through a trophozoite showing the trilayer membrane (TLM), microtubules (M), mitochondria (MT), inclusions (I), amylopectin granules (AM), unknown organelles (O). **C.** High-magnification image showing Golgi apparatus (G), lipids (L), amylopectin granules (AM), as well as intracisternal granules (IG). **D.** High-magnification longitudinal image showing part of the trilayer membrane (TLM) and microtubules (M). Also visible are amylopectin granules (AM), mitochondria (MT), and unknown organelles (O). Scales: A = 2 μm, B = 1 μm; C = 1 μm; D = 300 nm.

with *S. pisinnus* and *S. orientale* (Eastern Pacific). *Selenidium planusae* n. sp. branched in a clade with *S. fallax*. *Trollidium akkeshiense* n. gen. n. sp. branched in a novel clade, together with four environmental sequences. The clade containing *T. akkeshiense* n. gen. n. sp. was a sister group to *Polyplicarium*, but this relationship had low statistical support. Throughout the 18S rDNA tree, support was low at deeper nodes in the tree; support was generally higher nearer the tips, with a few exceptions (Fig. 13).

In the 28S rDNA dataset, the *Selenidium* in this study were split into two well-supported clades. *Selenidium planusae* n. sp. branched with *S. validusae* n. sp., *S. pherusae*, and *S. pygospionis* (Supplementary Material Fig. S1). *Selenidium*

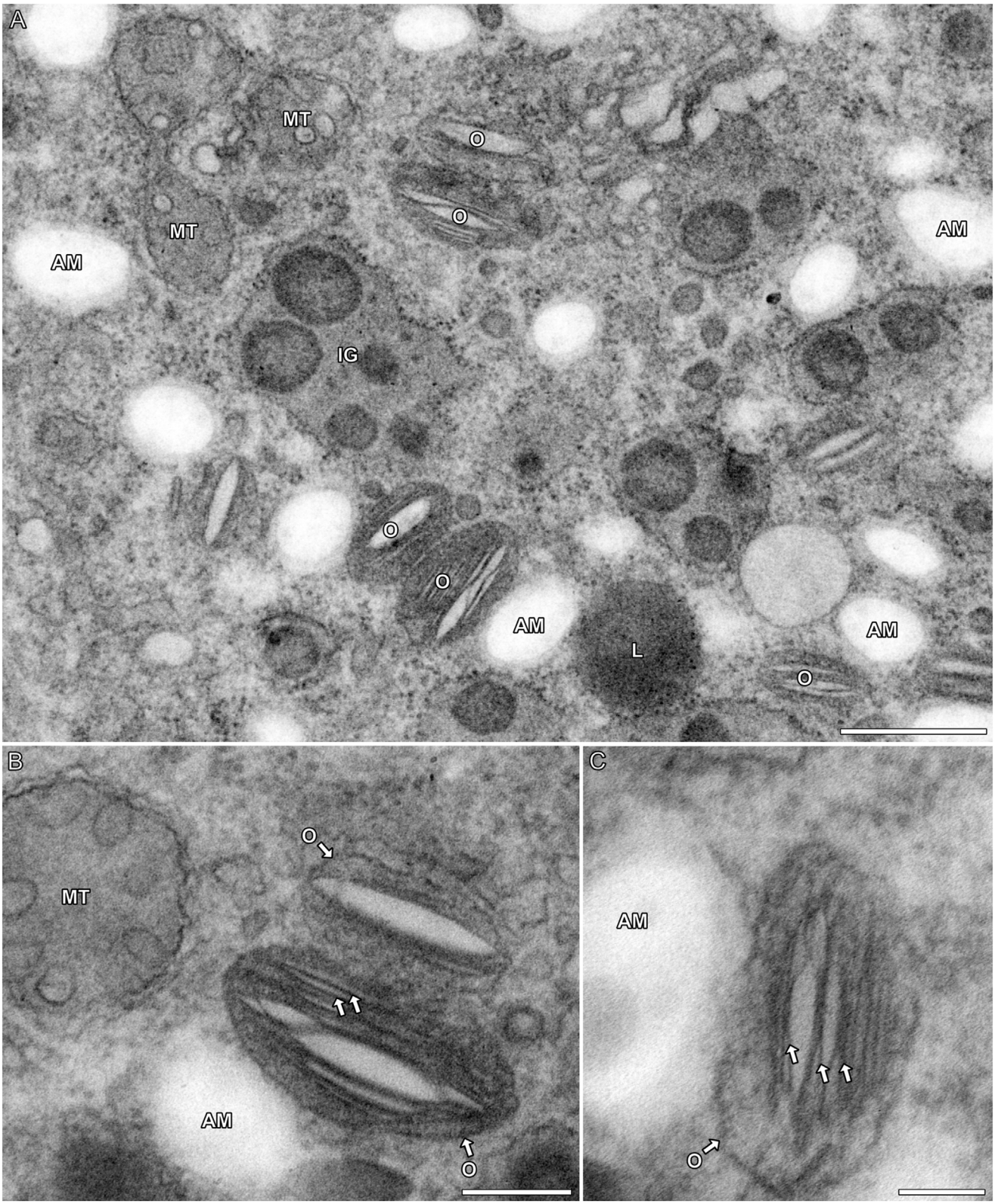

Figure 6. Transmission electron micrographs of *Selenidium validusae* n. sp. **A.** High-magnification image showing amylopectin granules (AM), mitochondria (MT), lipids (L), unknown organelles (O) and intracisternal granules

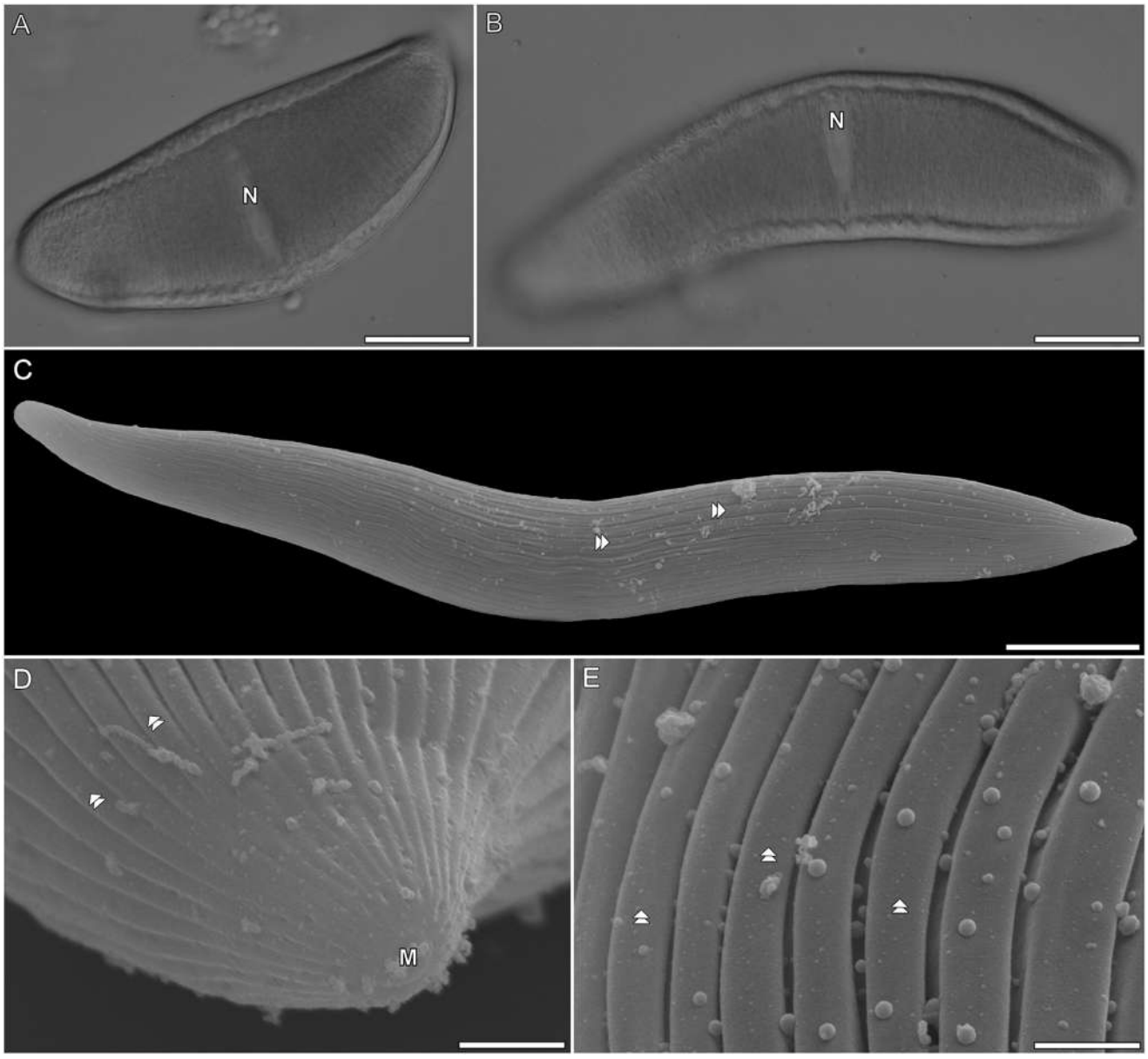

Figure 7. Light micrographs and scanning electron micrographs of *Selenidium pyroidea* n. sp. **A, B.** Light micrographs showing the general morphology of trophozoites with a central nucleus (N). **C.** Scanning electron micrograph of a trophozoite with the mucron oriented to the right. Folds on the surface of the cell (epicytic folds) are visible (double arrowhead). **D.** High-magnification scanning electron micrograph of the mucron (M). Epicytic folds (double arrowhead) are also visible near the mucron. **E.** High-magnification image showing epicytic folds (double arrowhead). Scales: A–C = 20 μm; D, E = 1 μm.

(IG). **B, C.** High-magnification image showing unknown organelles (O) next to mitochondria (MT) and amylopectin granules (AM). Note the thread-like composition (arrows) of unknown organelles. Scales: A = 1 μm; B = 500 nm; C = 200 nm.

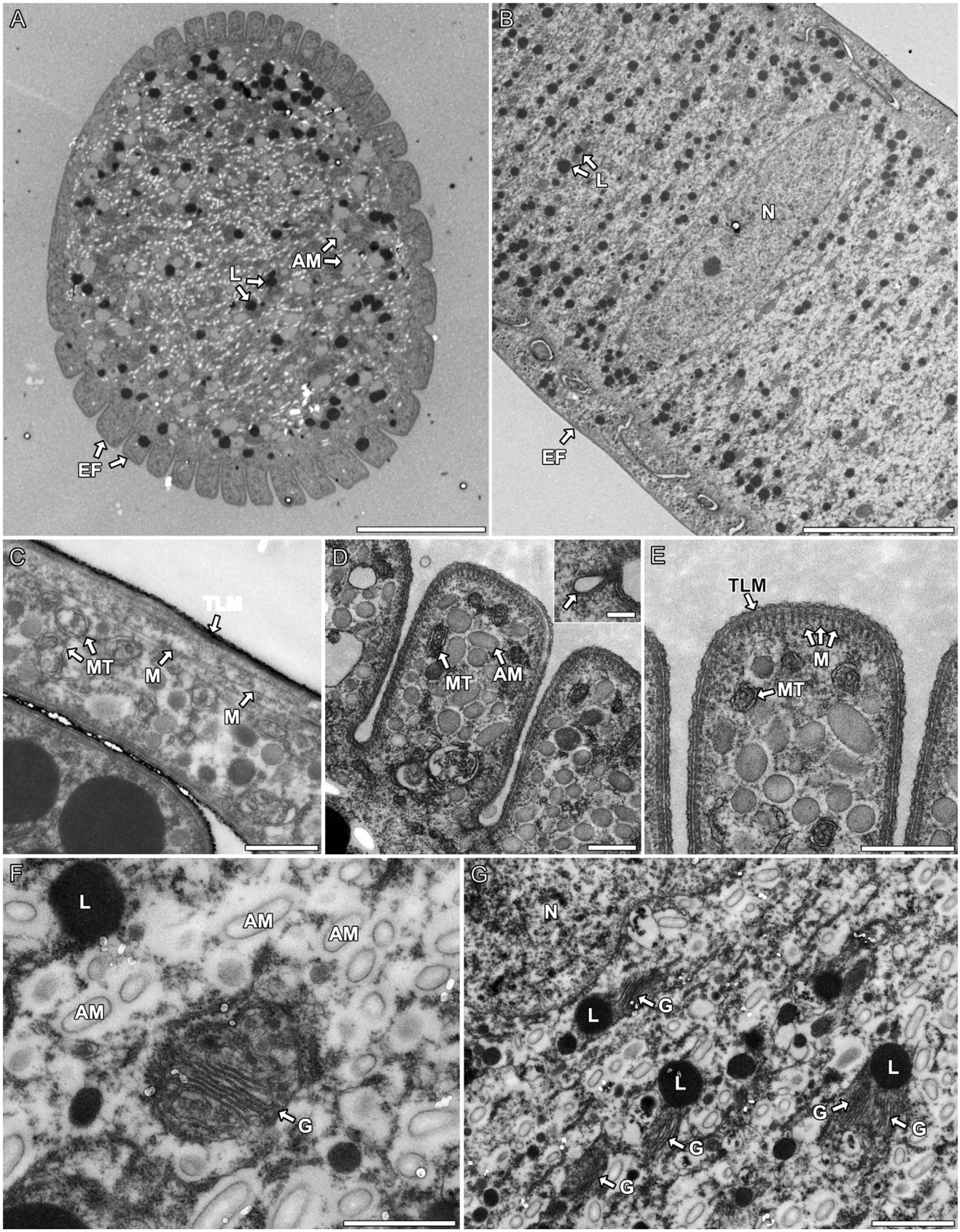
A
AM
L
EF
B
L
N
EF
C
TLM
MT
M
M
D
MT
AM
E
TLM
M
MT
F
L
AM
AM
AM
G
G
N
L
G
L
L
G
G
G
G

pyroidea n. sp. branched together with *S. orientale*. *Trollidium akkeshiense* n. gen. n. sp. was on a long branch, sister to *Gregarina* spp. and gregarine from crustaceans. Support at this node, and throughout deeper nodes in the tree was generally low (Supplementary Material Fig. S1).

A concatenated rDNA dataset was comprised of combined rDNA data including the four *Selenidium* from this study and *Trollidium akkeshiense* n. gen. n. sp., as well as all other gregarine apicomplexans for which data were available. In the analysis, *Selenidium* was split between two clades: 1) a clade consisting of *S. planusae* n. sp. and *S. validusae* n. sp., along with previously sequenced *Selenidium*, *S. pygospionis* and *S. pherusae*, and 2) a clade consisting of *Selenidium* from sipunculids, *S. orientale* and *S. pyroidea* n. sp. the relationship between these clades was unresolved (Fig. 14). *Ancora sagittata*, branched as a sister lineage to the clade containing *S. planusae* and *S. validusae* n. sp., albeit with low statistical support. *Trollidium akkeshiense* n. gen. n. sp. was a long branch together with a clade consisting of *Gregarina* spp., *Heliospora* and *Cephaloidophora*; support for this clade was low.

Discussion

Morphological and Molecular Comparisons of Novel Species of *Selenidium* and *Trollidium akkeshiense* n. gen. n. sp.

Selenidium planusae n. sp. was isolated from *Cirriformia tentaculata* Montagu, 1808. Previous studies have described at least two different species of *Selenidium*, *S. fallax* MacGregor and Thomasson, 1965 and *S. mackinnonae* Reichenow, 1932, from that same host (Levine 1971). These species, though, can be distinguished from *S. planusae* n. sp. based on the presence/absence of epicytic folds on the surface of trophozoites. While SEM observations of the surface of *S. planusae* n. sp. did show shallow folds, none of the cells ($n = 5$) viewed in cross-section under TEM showed any evidence of epicytic folds. Therefore, it was concluded that what was observed under SEM, was likely an artifact due to the cell constricting during the fixation. Epicytic folds are clearly visible on the surface of *S. fallax*, even in light micrographs (Rueckert and Horák 2017), and this is something that was never observed in *S. planusae* n. sp. Moreover, gamonts of *S. planusae* n. sp. had a caudo-frontal orientation in syzygy. The syzygy orientation of *S. mackinnonae* was described as being frontal (Supplementary Material Table S1). Molecular data (18S rDNA) is available for *S. fallax*. This isolate did branch together with *S. planusae* n. sp. in the 18S rDNA phylogenetic analyses. However, a pairwise comparison of the sequences showed only a 93% similarity, differing at 106 bases across 1,607 comparable positions.

Selenidium validusae n. sp. was isolated from *Acrocirrus validus* Marenzeller, 1879, a polychaete from which no other gregarine was found to have been isolated. The trophozoite stages of *S. validusae* n. sp. and *S. planusae* n. sp. are superficially similar. Both are compressed, translucent, and move (bend and twist) in a similar manner, and lack epicytic surface folds; and they were both isolated from the same sampling site, albeit from different host species. These two species, however, can be distinguished by their type of syzygy: *Selenidium planusae* n. sp. was found to have caudo-frontal syzygy, while *S. validusae* n. sp. exhibited caudal syzygy. Sequences from these two species also differed by 21% across 4,585 comparable sites. This was reflected in the phylogenetic analyses where *S. planusae* n. sp. and *S. validusae* n. sp. were either in separate clades (18S rDNA) or branched as well-supported sister lineages (concatenated dataset).

Figure 8. Transmission electron micrographs of *Selenidium pyroidea* n. sp. **A.** Cross-section of the trophozoite showing 37 epicytic folds, electron-dense lipids (L), as well as amylopectin granules (AM). **B.** Longitudinal-section through a trophozoite showing the nucleus (N), epicytic folds (EF), as well as electron-dense lipids (L). **C.** High-magnification longitudinal-section showing mitochondria (MT) and microtubules (M) underlaying the trilayer membrane (TLM). **D.** High-magnification cross-section showing an epicytic fold containing mitochondria (M) and amylopectin granules (AM). **D (inset).** High-magnification image showing surface mediated nutrition acquisition (arrow) at the base of an epicytic fold. **E.** Cross-section through an epicytic fold showing the trilayer membrane (TLM), microtubules (M), and mitochondria (MT). **F.** High-magnification image of Golgi apparatus (G), electron-dense lipids (L), and amylopectin granules (AM). **G.**High-magnification image of the cytoplasm showing the nucleus (N), lipids (L), and Golgi apparatus (G). Scales: A = 10 μm; B = 5 μm; C, D. = 1 μm; D (inset) = 50 nm. E, F = 500 nm; G = 1 μm.

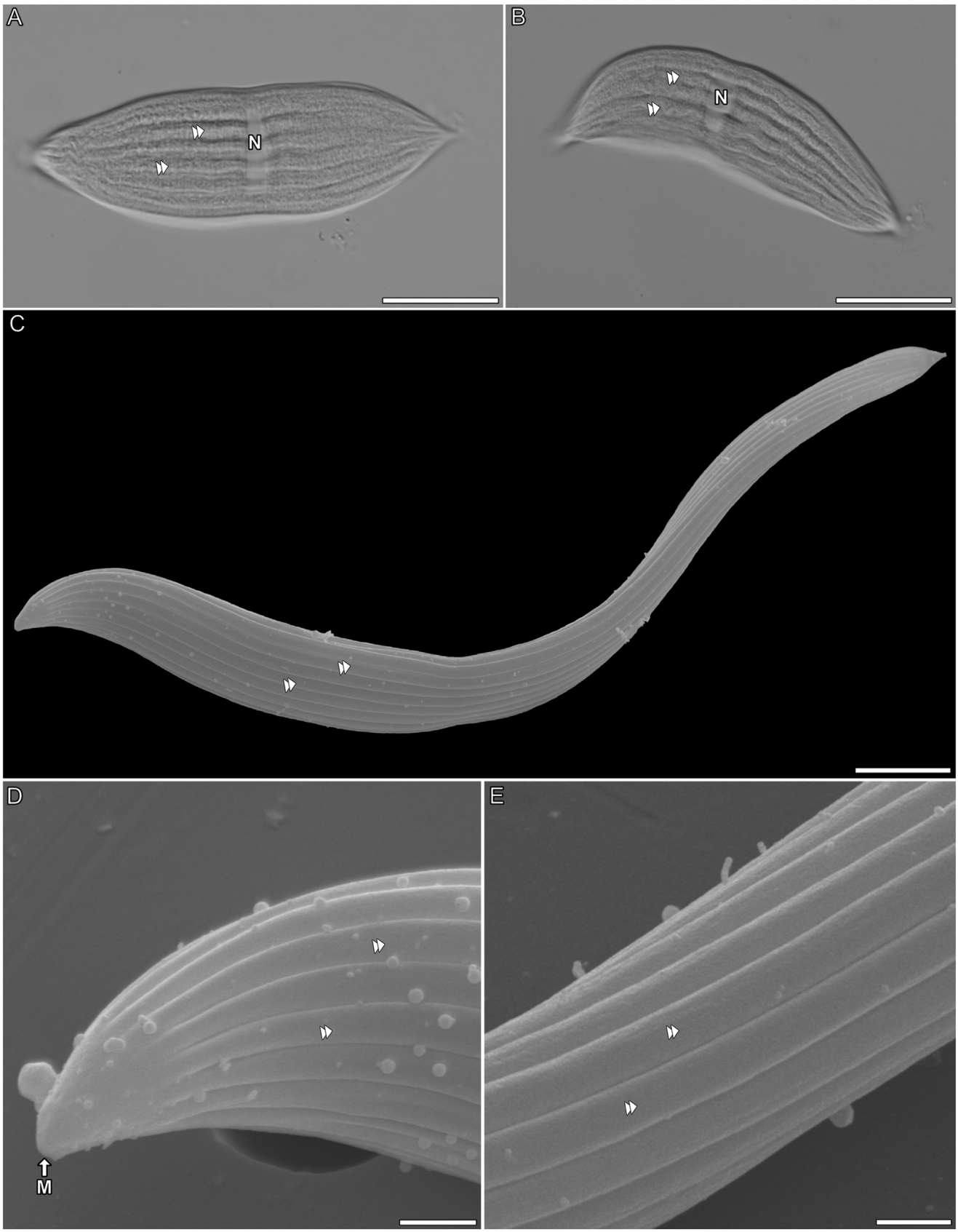
A
N
B
N
C
D
M
E

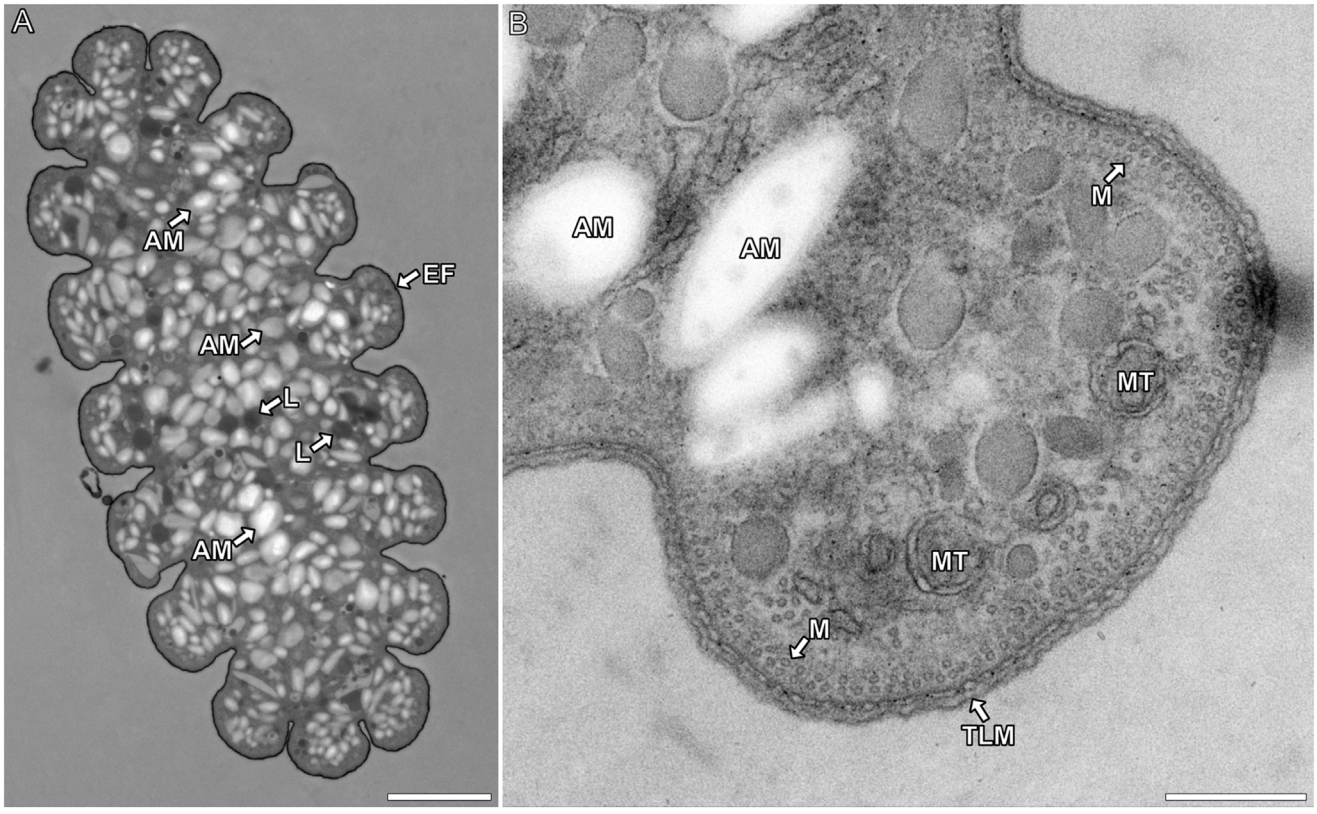

Figure 10. Transmission electron micrographs of *Selenidium orientale*. **A.** Cross-section of a trophozoite showing 17 epicytic folds (EF), lipids (L), amylopectin granules (AM). **B.** High-magnification cross-section of an epicytic fold (EF) with mitochondria (MT), amylopectin granules (AM), as well as the trilayer membrane (TLM) with microtubules (M). Scales: A = 5 μm; B = 500 nm.

Selenidium pyroidea n. sp. and *S. orientale* were both isolated from a sipunculid, *Themiste pyroides* Chamberlin, 1919. Three species of *Selenidium* have been described from sipunculids in the Western Pacific/Sea of Japan, namely *S. folium*, *S. siphonosomae* (Hukui 1939) and *S. orientale* (Bogolepova 1953). These three species, although from a geographically similar region, were isolated from different hosts (not *Themiste pyroides*). More recent work in the Eastern Pacific (Canada) did isolate *S. orientale* from *Themiste pyroides* (Rueckert and Leander 2009), providing the first molecular sequence for this species. It is possible that the *S. orientale* isolated from these different geographic regions (Russia, Japan, and Canada) represent two or three separate species. Nonetheless, molecular data is missing from the type locality (Peter the Great Bay, Russia), and there only appears to be limited morphological differences of the trophozoites between these locations. For example, Simdyanov and Kuvardina (2007) did TEM sectioning on *S. orientale* from its type locality and found 15 epicytic folds; the original description by Bogolepova (1953) reported 16 folds (note: without TEM imaging); and here 17 epicytic folds is reported on the surface of *S. orientale* from Japan (Supplementary Material Table S1). However, the 18S rDNA of *S. orientale* from Japan and the isolate

Figure 9. Light micrographs and scanning electron micrographs of *Selenidium orientale*. **A, B.** Light micrographs showing the general morphology of trophozoites with a central nucleus (N) and epicytic folds (double arrowheads). Mucrons are oriented to the left. **C.** Scanning electron micrograph of a trophozoite with the mucron oriented to the left. Folds on the surface of the cell (epicytic folds) are visible (double arrowhead). **D.** High-magnification scanning electron micrograph of the mucron (M). Epicytic folds (double arrowhead) are also visible near the mucron. **E.** High-magnification image showing epicytic folds (double arrowhead). Scales: A, B = 20 μm; C = 10 μm; D, E = 1 μm.

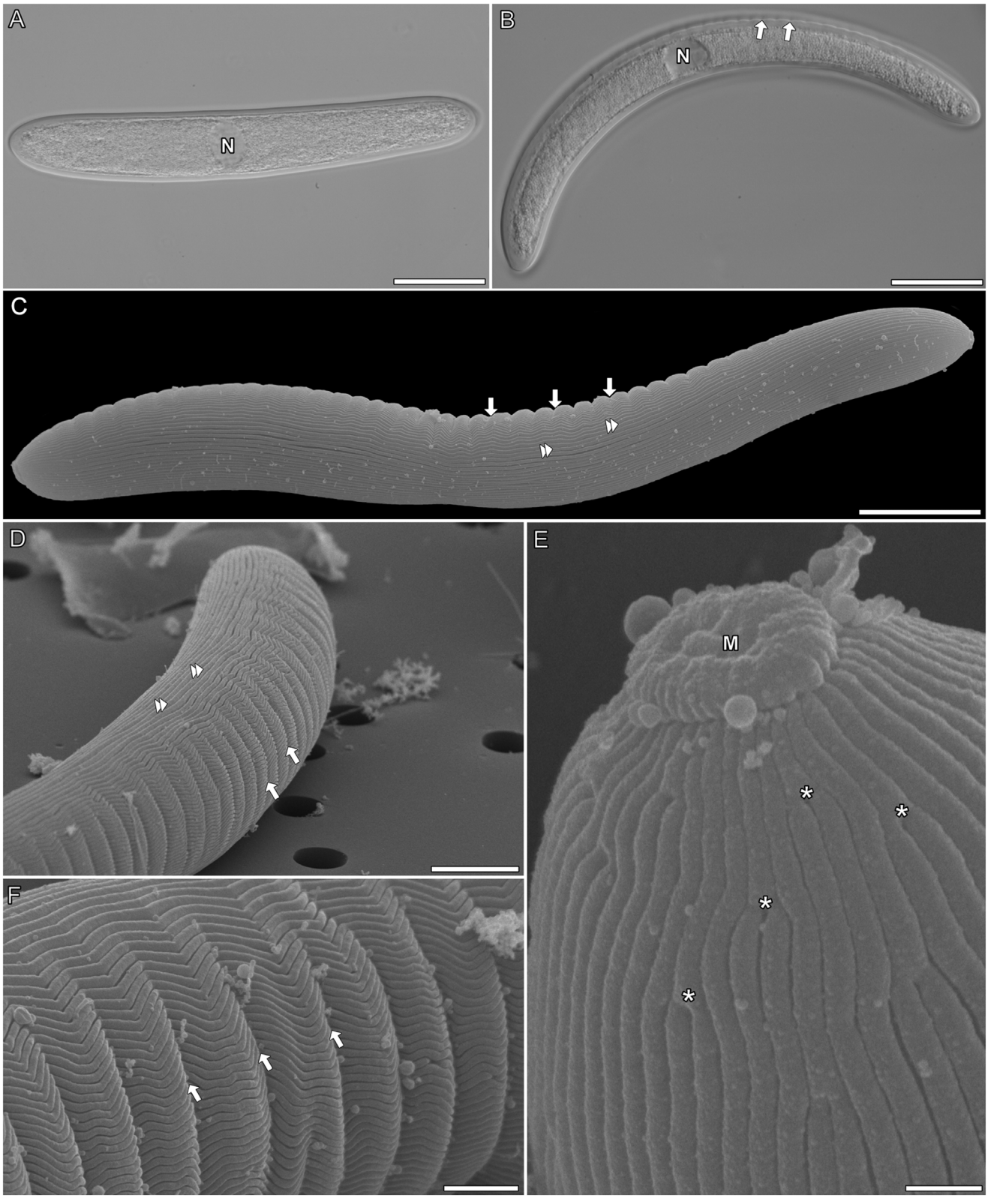
A
N
B
N
C
D
E
M
F

from Canada only differed by 2% across 1,693 comparable sites). Therefore, it was determined that it would be premature to establish a new species based on the information collected for *S. orientale* in this study, and likely this topic will have to be reexamined with more molecular data representing each locality. With regard to *S. pyroidea* n. sp., it was concluded that this represents a new species of *Selenidium*. It was considered a possibility that *S. pyroidea* n. sp. represented a more mature stage of *S. orientale*, however, isolates of *S. pyroidea* n. sp. can be distinguished from *S. orientale* and other *Selenidium* from sipunculids based on the number of surface folds (37). Moreover, the molecular sequences generated from *S. pyroidea* n. sp. and *S. orientale* differed by 14.1% across 4,800 comparable sites.

Trollidium akkeshiense n. gen. n. sp. represents a rather curious case. Superficially, this lineage is similar to *Selenidium* and other so-called archigregarines in that its trophozoite stage is elongate and moves by bending. However, the organization of microtubules under the trilayer membrane in *T. akkeshiense* n. gen. n. sp. is unique and is different from other *Selenidium*. Among members of the *Selenidium* (and other early-evolving marine alveolate lineages) it is typical to find microtubules subtending the membrane of the trophozoite stage (Desportes and Schrével 2013a). It is these microtubules that are thought to facilitate the bending and twisting movement of the parasite and have become a diagnostic characteristic uniting *Selenidium* and other early-evolving marine gregarine lineages (Mellor and Stebbings 1980; Stebbings et al. 1974). These microtubules typically run longitudinally, the length of the trophozoite, and are found around the entire circumference of the cell; in *T. akkeshiense* n. gen. n. sp., they are only found on one side of the trophozoite. *Trollidium akkeshiense* n. gen. n. sp. possesses a general bending and flicking pattern of movement. Videos taken of the cell movement shows this movement, repeating in the same direction (See Supplementary Video 1). These microtubules correspond to a unique zig-zag pattern of epicytic surface folds and is an example where the trilayered membrane of gregarines has formed unique shapes and structures that have a probable role in the life strategy of the parasite (e.g., nutrient acquisition or cell attachment/invasion etc.). Other examples include *Ditrypanocystis cirratuli*, a gregarine possessing an "undulating membrane" along the cell (Burt et al. 1963; MacGregor and Thomasson 1965), as well as and *Cuspissella ishikariensis* and *Loxomorpha harmoethoë*, gregarines that have "spikes" and modified folds on the surface of their mucrons (Iritani et al. 2018).

Two other gregarine species within the genus *Selenidium* have been described from the polychaete host *Pherusa plumose*, *S. curvicollum* (Bogolepova 1953) and *S. pherusae* (Paskerova et al. 2018). However, *T. akkeshiense* n. gen. n. sp. can be distinguished from these species based on 1) the number of surface folds (*T. akkeshiense* n. gen. n. sp. has 103 folds), 2) the organization of microtubules along only one side of the trophozoite, and 3) its phylogenetic position inferred from 18S rDNA. It is interesting to note that the sequence from *T. akkeshiense* n. gen. n. sp. did not group with these other two isolates of *Pherusa plumose*. Generally speaking, gregarines isolated from closely related hosts are infected with gregarines that are also closely related. Among *Selenidium*, this pattern can be seen among tube-forming polychaete hosts (e.g., serpulids, sabellids, and spionids) (Desportes and Schrével 2013a, b; Schrével et al. 2016). This pattern is intriguing and might serve as an interesting model for testing coevolution and cospeciation among gregarines and their hosts. At this juncture, *Trollidium akkeshiense* n. gen. n. sp., appears to represent an exception to this broad pattern.

The 18S rDNA of *Trollidium akkeshiense* n. gen. n. sp. was nested with robust support within a group of four marine environmental sequences. These sequences were generated from marine environments from sediments around deep-sea methane seeps in the East Pacific (Pasulka et al. 2016),

Figure 11. Light micrographs and scanning electron micrographs of *Trollidium akkeshiense* n. gen. n. sp. **A, B.** Light micrographs showing the general morphology of trophozoites with a central nucleus (N). Note that parts of the surface appear wrinkled (arrows); mucrons are oriented to the right. **C.** Scanning electron micrograph showing the general trophozoite morphology. The mucron is oriented to the right. Epicytic folds (double arrowheads) are visible on the surface. The surface, particularly in the middle of the cell is wrinkled (arrows). **D.** Micrograph showing the epicytic folds (double arrowheads) and the wrinkled surface (arrows). **E.** High-magnification micrograph of mucron (M), as well as the bifurcations of the epicytic folds (asterisks). **F.** High-magnification micrograph of the wrinkled region of the epicytic folds (arrows). Note that the folds in this region appear to zig-zag. Scales: A–C = 20 μm; D = 5 μm; E = 500 nm; F = 2 μm.

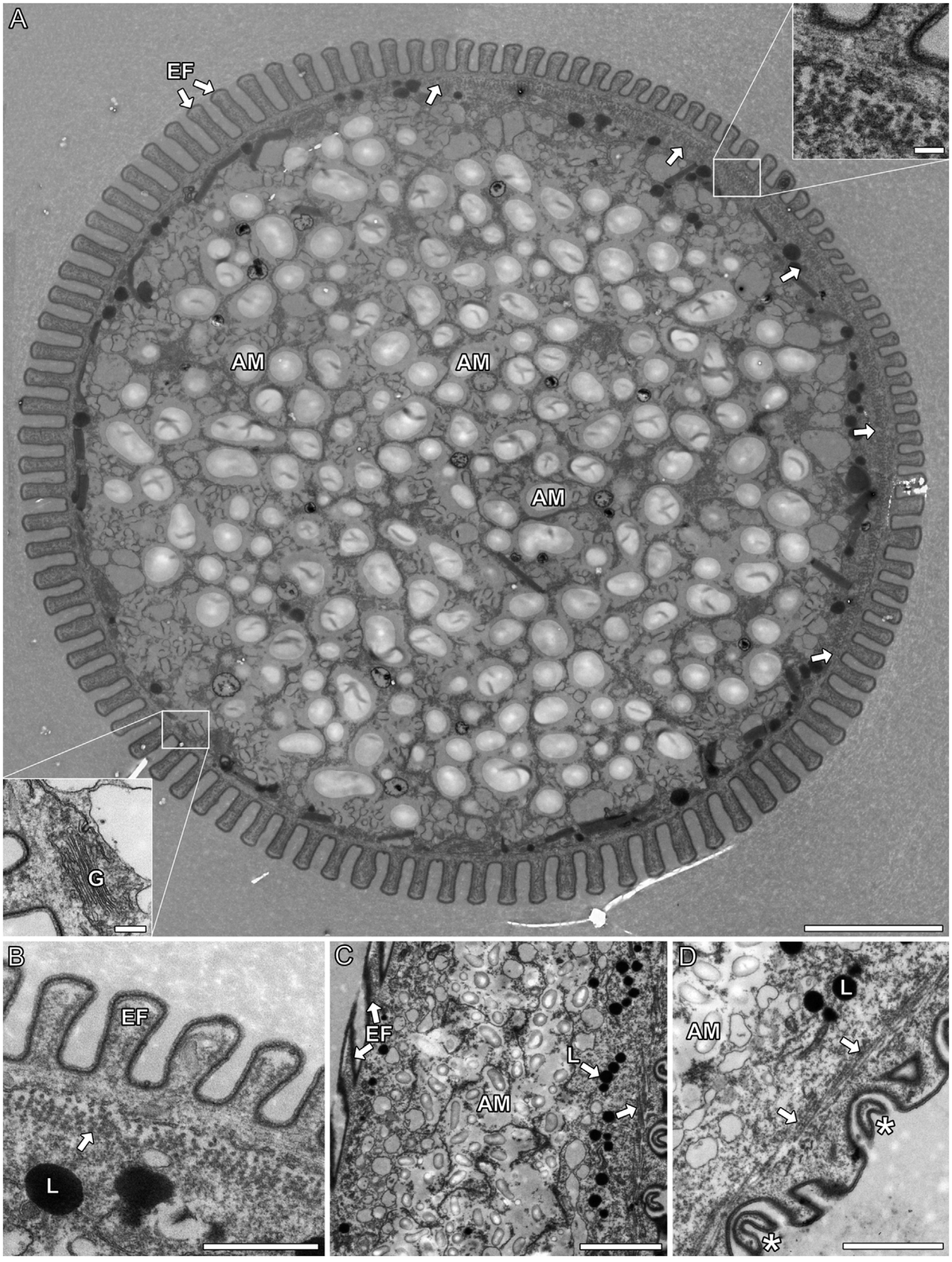
A
EF
AM
AM
AM
G
B
EF
L
C
EF
L
AM
D
L
AM
*
*

cold-seep sediments in the West Pacific, and the Western Green Arctic (Stoeck et al. 2007). The clade containing the sequence from *T. akkeshiense* n. gen. n. sp. and the environmental sequences did not have any statistical support to any known gregarine group; and a similar result was also present in the concatenated molecular datasets. Therefore, there was little that could be concluded from the phylogenetic position of this novel lineage of marine gregarine based on ribosomal data.

Based on the data we have collected for *T. akkeshiense* n. gen. n. sp., the classification of this lineage as either an archigregarine or eugregarine is ambiguous. On the one hand, *T. akkeshiense* n. gen. n. sp. has an elongated trophozoite stage that bends in a fashion similar to archigregarines. On the other hand, *T. akkeshiense* n. gen. n. sp. has an organization of microtubules that is quite unique when compared to other known archigregarines and has a long-branching ribosomal sequence – long-branching sequences are rare among archigregarine lineages; the only exception being *Platyproteum* and *Filipodium* (Rueckert and Leander 2009). However, it seems even *Platyproteum* and *Filipodium* are not even gregarines (Mathur et al. 2019). This being the case, it was determined to classify *T. akkeshiense* n. gen. n. sp. as a eugregarine, with the understanding that future work (likely transcriptomic sequencing) would help clarify the evolutionary position of this lineage.

Bizarre Organelles in *Selenidium planusae* n. sp. and *S. validusae* n. sp.

One of the more intriguing findings was the presence of ovular organelles measuring 300 nm in length that were distributed throughout the cytoplasm of *S. validusae* n. sp. These objects varied little in morphology and were commonly found in all trophozoite cells collected from different host individuals and samplings. They were striated with numerous longitudinal-running fibrils. No parallel was found when searching the literature for comparable organelles or structures in gregarines, or other apicomplexans. The breakdown of ingested particles (nutrients) in gregarines has been documented in *Selenidium* (Desportes and Schrével 2013a; Schrével 1971a, b). These inclusions have many visible "whorls"; and while we did identify inclusion-whorls within *S. validusae* n. sp. these structures were not consistent with regard to the shape, size, or abundance of the organelle in question. Additionally, if these were digestive organelles, vacuoles or inclusions, one would expect to see more variability, representing stages of digestion. These organelles, however, varied little in size and appearance when compared to each other. The longitudinal fibrils are reminiscent of thylakoids (of plastids), although membranes are not visible due to the relatively small size of the organelle. Likely a different fixation method is needed in order to study the membranes of such small structures. Moreover, the morphology of these organelles lack four discernable membranes and the appearance is not generally consistent with other known apicoplasts from apicomplexans or those belonging to other gregarines (Schrével 1971b; Tomova et al. 2006; Wakeman et al. 2014). However, if indeed these are some type of relic plastid, their distinct morphology to that of other known apicoplasts might hint at an independent evolutionary line of plastids in the ancestors of some gregarine apicomplexans. Although it must be conceded that this is largely speculation, given only the ultrastructural data presented in this study, the presence of such bizarre organelles is intriguing and merits further investigation.

Relationships Among *Selenidium*, and Phylogeny of Gregarines Using Ribosomal Datasets: Relics of Long Branch Attraction

In 18S rDNA phylogenies of the genus *Selenidium*, the group branches into four clades: 1) a clade containing the type species, *S. pendula*, 2) a

Figure 12. Transmission electron micrographs of *Trollidium akkeshiense* n. gen. n. sp. **A.** Cross-section of a trophozoite showing 103 epicytic folds (EF), and amylopectin granules (AM). Note that there is a region of the cell that contains microtubules (arrows), and this region does not fully encompass the trophozoite. **A (inset, top right).** A high-magnification image showing microtubules. **A (inset, bottom left)**. A high-magnification image showing the opposite side of the cell where microtubules are not observed. **B.** Cross-section through a trophozoite showing the bundle of microtubules (arrow) and a lipid (L) below the epicytic folds. **C.** A tangential-section showing epiphytic surface folds (EF), amylopectin granules (AM) and lipids (L), as well as microtubules (arrow) running longitudinally. **D.** A high-magnification image of the zig-zag patter of epicytic folds (asterisk) that correspond.to the microtubules (arrow), as well as lipids (L) and amylopectin granules. Scales: A = 3 μm (insets = 100 nm); B = 500 nm; C = 2 μm; D = 500 nm.

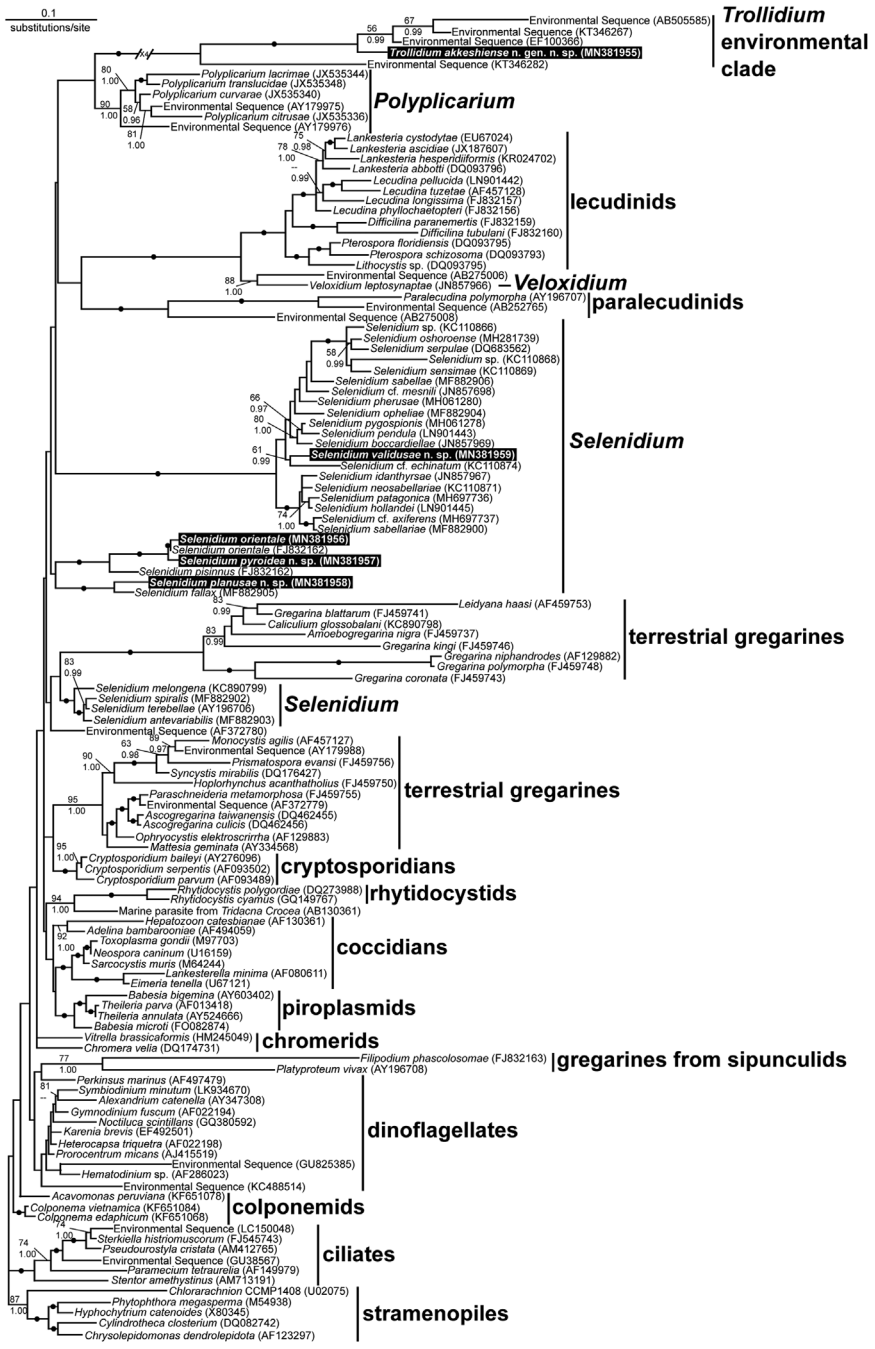

Figure 13. Maximum-likelihood (ML) tree inferred from 18S rDNA sequences. Maximum-likelihood bootstrap values over 50% and Bayesian posterior probabilities (PP) over 0.50 are shown at the nodes (ML/PP). Black dots indicate maximal support (100/1.00). The scale bar represents inferred evolutionary distance in changes/site. The novel sequences generated in this study are highlighted in bold font and black boxes.

clade isolated from sipunculids, 3) a clade isolated from cirratulid polychaetes, and 4) a clade isolated from terebellid polychaetes (Paskerova et al. 2018; Rueckert and Horák 2017). Each clade has robust statistical support, however, the relationship between each of the *Selenidium* clades is uncertain.

Prior to this study, only two 28S rDNA sequences have been generated from *Selenidium*: *S. pherusae* and *S. pygospionis* (Paskerova et al. 2018); in

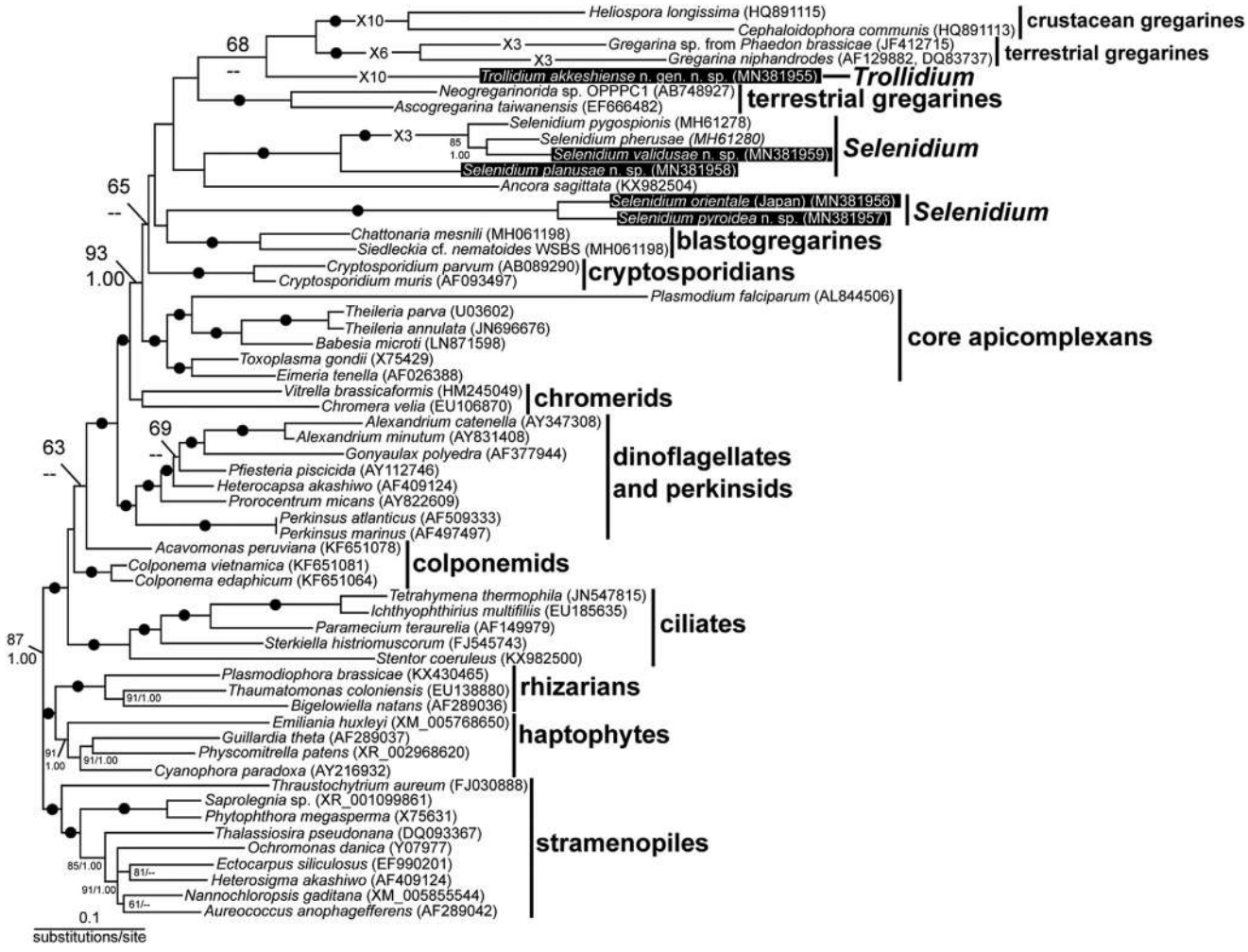

Figure 14. Maximum-likelihood (ML) tree inferred from concatenated 18S and 28S rDNA datasets. Maximum-likelihood bootstrap values over 50% and Bayesian posterior probabilities (PP) over 0.50 are shown at the nodes (ML/PP). Black dots indicate maximal support (100/1.00). The scale bar represents inferred evolutionary distance in changes/site. The novel sequences generated in this study are highlighted in bold font and black boxes.

the 18S rDNA dataset, both of these species belong to the clade containing the type species, *S. pendula*. Due to this limited sampling, one of the aims of this study was to improve the representation of *Selenidium* in the 28S rDNA datasets to address relationships among members of this group. This study was able to generate four additional *Selenidium* 28S rDNA sequences that included representatives of *Selenidium* from sipunculids, and cirratulid polychaetes. As result, two of the *Selenidium* lineages (from cirratulids and the clade containing *S. pendula*) that were previously unresolved in 18S rDNA trees were robustly supported in a single clade. This group was sister to *Ancora sagitatta*, a more derived lineage, to the exclusion of *Selenidium orientale* and *S. pyroidea* n. sp., but nodal support was low for this relationship, and it is also possible that this topology is a result of long branch attraction. It was therefore concluded that splitting *Selenidium* into separate genera was not justified at this point in time, due to a lack of resolution between *Selenidium* in the tree.

Relationships/topologies between gregarines and other apicomplexan groups in concatenated rDNA analyses should be treated with a certain degree of skepticism. Some of the topology in these trees is likely a relic issue of quickly evolving sequences, resulting from long branch attraction between some of these lineages (e.g., *Trollidium akkeshiense* n. gen. n. sp., *Cephaloidophora*, and

Gregarina). The first 28S rDNA sequence data that had been collected from gregarines showed promise in resolving some of the deeper nodes in the tree (Simdyanov et al. 2017; Paskerova et al. 2018). However, select nodes in these datasets (and even in the present study) are questionable, for instance, the position of *Cryptosporidium* at the base of gregarines. While it is apparent that statistical support for a limited number of gregarine groups has increased, it can be argued that these statistical values and the general topology of the trees as a whole are influenced by long branch attraction and a limited taxon sampling. A similar pattern can be seen in some of the first gregarine 18S rDNA trees, where a limited number of taxa resulted in low/moderate bootstrap support between groups (e.g., lecudinids and *Selenidium*) (Rueckert and Leander 2008, 2009). In contemporary 18S rDNA datasets that are more taxon rich, support for these relationships has waned and the topologies have since changed (Paskerova et al. 2018; Rueckert and Horák 2017). A similar pattern seems likely to emerge as more 28S rDNA sequences become available. From this, it seems apparent that larger datasets, likely those from multiple protein-coding genes, will be needed to infer deep relationships in this group.

Taxonomic Summary

Phylum: Myzozoa Cavalier-Smith and Chao, 2004

Subphylum: Apicomplexa Levine, 1970

Order: Archigregarinorida, Grassé, 1953

Family Selenidiidae Brasil, 1907

Genus *Selenidium* Giard, 1884

Selenidium planusae n. sp. Wakeman, 2019

Description Trophozoites elongate with an average length and width of 124 μm and 27 μm, respectively. Cells appear compressed in cross-section, with an average thickness of 10 μm. Nucleus spherical or ovoid with an average width of 7 μm and length of 10 μm. Trophozoites lacked obvious epicytic folds on the surface. Mucron nipple-like, narrowing to a point. Syzygy caudo-frontal. Movement by bending and thrashing. Microtubules observed subtending trilayer membrane.

Type host *Cirriformia tentaculata* Montagu, 1808 (Annelida, Polychaeta, Cirratulidae)

Location in host Intestinal lumen

Iconotype Fig. 1A

Hapantotype Trophozoites on SEM stubs with a gold sputter coat have been stored in the algal and protist collection in the Hokkaido University Museum (KCW_Selenidiumplanusae_1).

LSID BCBE6D99-FC92-48C5-863C-847AC38232E0

Etymology The species name, *planusae*, refers to flat/compressed appearance of the trophozoites in cross-section.

Selenidium validusae n. sp. Wakeman, 2019

Description Trophozoites elongate with an average length and width of 178 μm and 31 μm, respectively. Cells appear compressed in cross-section, with an average thickness of 15 μm. Nucleus ovoid with an average width of 10 μm and length of 13 μm. Trophozoites lacked obvious epicytic folds on the surface. Mucron nipple-like, narrowing to a point. Dense refractive rhoptries observed near the mucron. Syzygy caudal. Movement by bending and thrashing. Microtubules observed subtending trilayer membrane. Electron-dense organelles with unknown function, striated with longitudinal fibrils measuring 175 nm × 300 nm observed throughout cytoplasm.

DNA sequence 18S rDNA sequence 28S rDNA sequence (GenBank MN381959).

Type locality Oshoro, Hokkaido, Japan (43°12'33.26Ñ 140°51'30.67Ë). Host commonly found on the underside of large (~0.5 m diameter) rocks in the low intertidal to subtidal zones.

Type habitat Marine

Type host *Acrocirrus validus* Marenzeller, 1879 (Annelida, Polychaeta, Acrocirridae)

Location in host Intestinal lumen

Iconotype Fig. 1A

Hapantotype Trophozoites on SEM stubs with a gold sputter coat have been stored in the algal and protist collection in the Hokkaido University Museum (KCW_Selenidiumvalidusae_1).

LSID BCBE6D99-FC92-48C5-863C-847AC38232E0

Etymology The species name, *validusae*, refers to the host species, *Acrocirrus validus*, from which the apicomplexan was isolated.

Selenidium pyroidea n. sp. Wakeman, 2019

Description Trophozoites elongate with an average length and width of 309 μm and 35 μm, respectively. Cells appear circular in cross-section, with an average thickness of 39 μm. Nucleus ovoid with an average width of 30 μm and length of 9 μm. Trophozoites with 37 epicytic folds. Mucron narrowed but generally rounded. Movement by slow bending. Microtubules observed subtending trilayer membrane.

DNA sequence 18S rDNA sequence 28S rDNA sequence (GenBank MN381957).

Type locality Akkeshi, Hokkaido, Japan (43°01'06.29Ñ 144°50'01.4Ë). Host commonly found entangled in the rhizome of seagrass in the low intertidal to subtidal zones.

Type habitat Marine

Type host *Themiste pyroides* Chamberlin, 1919 (Sipuncula, Themistidae)

Location in host Intestinal lumen

Iconotype Fig. 1A

Hapantotype Trophozoites on SEM stubs with a gold sputter coat have been stored in the algal and protist collection in the Hokkaido University Museum (KCW_Selenidiumpyroidea_1).

LSID BCBE6D99-FC92-48C5-863C-847AC38232E0

Etymology The species name, *pyroidea*, refers to the host species, *Themiste pyroides*, from which the apicomplexan was isolated.

Phylum: Myzozoa Cavalier-Smith and Chao, 2004

Subphylum: Apicomplexa Levine, 1970

Order: Eugregarinorida, Léger, 1900

Family Lecudinidae Kamm, 1922

Genus *Trollidium* n. gen. Wakeman, 2019

Description Trophozoites elongate with a bending/flicking movement. Epicytic folds on certain areas of the surface wrinkle/zig-zag, corresponding to microtubules underneath the surface of the membrane; microtubules extend down only one side of the trophozoite. Mucron and posterior end rounded.

Type species Trollidium akkeshiense

Etymology The generic name, *Trollidium*, is in reference to a famous brand of gummy worms, Trolli, which also appear wrinkled on their surface, and generally resemble the trophozoites of the type species as a whole.

Trollidium akkeshiense n. sp. Wakeman, 2019

Description Trophozoites elongate with an average length and width of 218 μm and 20 μm, respectively. Cells appear circular in cross-section, with an average thickness of 20 μm. Nucleus ovoid with an average width of 14 μm and length of 17 μm. Trophozoites with 103 epicytic folds. Parts of the epicytic folds zig-zag on the surface, giving a wrinkled appearance. Mucron generally rounded. Movement by bending/twitching. Microtubules observed subtending only one side of the trophozoite cell.

DNA sequence 18S rDNA sequence 28S rDNA sequence (GenBank MN381955).

Type locality Akkeshi, Hokkaido, Japan (43°01'06.29Ñ 144°50'01.4Ë). Host commonly found entangled in the rhizome of seagrass in the low intertidal to subtidal zones.

Type habitat Marine

Type host *Pherusa plumosa* Müller, 1776 (Annelida, Polychaeta, Flabelligeridae)

Location in host Intestinal lumen

Iconotype Fig. 1A

Hapantotype Trophozoites on SEM stubs with a gold sputter coat have been stored in the algal and protist collection in the Hokkaido University Museum (KCW_Trollidiumakkeshiense_1).

LSID BCBE6D99-FC92-48C5-863C-847AC38232E0

Etymology The species name, *akkeshiense*, refers to the locality, Akkeshi, Hokkaido, Japan, from which the apicomplexan was isolated.

Methods

Collection of hosts and isolation of parasites: *Cirriformia tentaculata* Montagu, 1808, *Acrocirrus validus* Marenzeller, 1879, *Pherusa plumosa* Chamberlin, 1919, and *Themiste pyroides* Chamberlin, 1919 were collected between April – August 2018 from rocks near the Oshoro Marine Station, Oshoro, Hokkaido, Japan (43°12'33.26Ñ 140°51'30.67Ë) and Akkeshi Marine Station, Akkeshi, Hokkaido, Japan (43°01'06.29Ñ 144°50'01.4Ë). Worms were held in cool seawater and transported to the laboratory where their intestines were dissected out using forceps and razors. Between 20 and 30 of each host species were collected and dissected; all were infected with a single species of gregarine parasite, with the exception of *T. pyroides* which was infected with two species (*Selenidium pyroidea* n. sp. and *S. orientale*). Parasites were found in all individual hosts. Feeding stages (trophozoites) were isolated using hand-drawn glass pipettes, and subsequently washed (until clean) in filtered, autoclaved seawater for further morphological and molecular analysis.

Light microscopy, scanning electron microscopy and transmission electron microscopy: Differential interference contrast (DIC) images and videos were taken using a Zeiss Axioscope 2 *Plus* microscope connected to a Leica MC 120 HD (Wetzlar, Germany) or a Canon EOS Kiss X8i camera (Tokyo, Japan). For scanning electron microscopy, individuals were transferred to a 3 μm or 40 μm mesh in 2.5% glutaraldehyde in seawater on ice for 15 min. After washing the samples three times for 5 min in seawater, the mesh was placed in 1% OsO_4 for 30 min, and subsequently washed with distilled water and dehydrated through a graded series of ethanol (30%, 50%, 75%, 80%, and 100%) for 5 min at each step. Samples were critical point dried with CO_2, sputter-coated with 5 nm gold and viewed using a Hitachi N-3000 SEM. For transmission electron microscopy, individual cells were fixed in 2.5% glutaraldehyde in seawater on ice for 30 min, washed in seawater, and post fixed with 1% OsO_4 on ice for 1.5 hours; both fixation steps were performed in the dark. Following the fixation with OsO_4, samples were washed in seawater, and dehydrated through a graded

series of ethanol (30%, 50%, 75%, 80%, and 100%) for 5 min at each step, and subsequently moved to a 1:1 acetone/ethanol mixture and a 100% acetone solution for 10 min each. Samples were then placed in a 1:1 resin (Agar Low Viscosity Resin, Agar Sciences)/acetone mixture for 30 min, followed by 100% resin overnight at room temperature. Resin was exchanged the following day, and samples were polymerized at 68 °C for 32 hours. Samples were cut with a diamond knife and viewed with a Hitachi-7400 TEM.

DNA extraction, PCR amplification, and sequencing of 18S rDNA: Single-cell isolates of each parasite were placed in 0.2 ml PCR tubes. Total genomic DNA was extracted following the manufacturers protocol using an Epicentre FFPE extraction kit (Epicentre, Madison, Wisconsin, USA). The primers PF1 and SSUR4, were initially used to amplify 18S rDNA using the following protocol on a thermal cycler: Initial denaturation 95 °C 5:00 min; 35 cycles of 95 °C 0:30 s, 52 °C 0:30 s, 72 °C 2:00 min; final extension 72 °C 7:00 min. Subsequently, 1 μl of the initial PCR relation was used in a second PCR with PF1-1281R and 671F-SSUR4 under the following parameters: Initial denaturation 95 °C 5:00 min; 25 cycles of 95 °C 0:30 s, 52 °C 0:30 s, 72 °C 1:40 min; final extension 72 °C 7:00 min. To amplify 28S rDNA sequences, the primers 1700F-28S1483R and D3A-28S3000R were used in an initial PCR to amplify the ITS regions as well as 28S rDNA using the following program on a thermocycler: 95 °C 5:00 min; 25 cycles of 95 °C 0:30 s, 52 °C 0:30 s, 72 °C 2:30 min; final extension 72 °C 7:00 min. Subsequently, 1 μl of these initial PCR reactions were used in a second round of amplifications using the primer pairs 25R1-1700 F, 25F1-LSU R2 (off 1700F-28S1483R), and LSU2200F-LSU3000R, and LSU D3A-LSU R2 (off LSU D3A-28S3000R) following the program on a thermocycler: Initial denaturation 95 °C 5:00 min; 25 cycles of 95 °C 0:30 s, 52 °C 0:30 s, 72 °C 2:30 min; final extension 72 °C 7:00 min. In each PCR reaction, Econotaq 2X Mastermix (Lucigen, Middleton, USA) was used, following the manufacturer's protocols. PCR products were purified using a Qiagen PCR purification kit (Qiagen, Germantown, USA); 1 μl of purified product was used in a sequencing reaction with ABI BigDye Terminator v1.1 (Applied Biosystems, Massachusetts, USA) and subsequently purified with ethanol, before being eluted in 18 μl Hi-Di Formamide (Applied Biosystems, Massachusetts, USA) and sequenced on a 3130 Genetic Analyzer (Applied Biosystems, Massachusetts, USA). The five novel sequences generated in this study were deposited in NCBI's GenBank (MN381955–MN381959). All primers used in this study are listed in Supplementary Table 2.

Phylogenetic analyses: New sequences generated in this study were identified by BLAST. Three molecular phylogenetic datasets were generated and viewed using Mesquite 3.6 (Maddison and Maddison 2015): 1) an 18S rDNA alignment (124 taxa) 2) a 28S rDNA alignment (63 taxa); and 3) a concatenated 18S + 28S rDNA alignment (58 taxa). MUSCLE (Edgar 2004) was used to align all datasets used for phylogenetic analyses. Gaps and highly variable regions were omitted using Gblocks (Castresana 2000; Talavera and Castresana 2007); final alignments used for phylogenetic analyses included 1,332, 2,829, and 4,507 bp for 18S rDNA, 28S rDNA, and the concatenated datasets, respectively.

The best-fit model for each dataset was selected using IQ-TREE under AICc (Trifinopoulos et al. 2016). Maximum-likelihood analyses on the three datasets were subsequently run with IQ-TREE using GTR + F + R10; GTR + F + R10, and GTR + F + R6, as the model of evolution for the 18S rDNA, 28S rDNA, and the concatenated 18S + 28S rDNA datasets, respectively; each analysis ran for 500 bootstrap pseudoreplicates.

All Bayesian analyses were performed using the program MrBayes 3.2.5 (Ronquist and Huelsenbeck 2003). The program was set to operate with GTR + I + G, and four Monte Carlo Markov Chains (MCMC) starting from a random tree. A total of 6,500,000, 7,000,000 and 150,000,000 runs were completed for 18S, 28S and concatenated (18S + 28S rDNA) datasets, respectively. Generations were calculated with trees sampled every 100 generations and the first 65,000 75,000 and 1,500,000 trees in each run were discarded as burn-in. When the standard deviation of split frequencies fell below 0.01, the program was set to terminate. Posterior probabilities correspond to the frequency at which a given node was found in the post-burn-in trees.

Declaration of Interests

The authors declare that they have no known competing financial interests or personal relationships that could have appeared to influence the work reported in this paper.

Acknowledgements

This work was supported by Japanese Society for the Promotion of Science (JSPS) grants 18K14774 and PG6R180004 to the author, as well funds and support provided by the Institute for the Advancement of Higher Education. Samples were collected with the kind support of Akkeshi Marine Station and Oshoro Marine Station. Generous support for the critical point drying of samples and access to a critical point dryer was provided by the Research Faculty of Agriculture at Hokkaido University. The author would also like to thank Timur Simdyanov and Gita Paskerova for graciously supplying copies of hard-to-find literature for reference.

Appendix A. Supplementary Data

Supplementary material related to this article can be found, in the online version, at doi:https://doi.org/10.1016/j.protis.2019.125710.

References

Adl SM, Bass D, Lane CE, Lukeš J, Schoch CL, et al. (2019) Revisions to the classification, nomenclature, and diversity of Eukaryotes. J Eukaryot Microbiol **66**:4–119

Burt DRR, Denny M, Thomasson PA (1963) On *Ditrypanocystis cirratuli* gen. nov., sp. nov. a gregarine possessing undulating membranes. Parasitiology **53**:12P

Bogolepova II (1953) Gregarines from the Peter the Great Bay. Tr Zool Inst Acad Nauk SSSR (Proc Zool Inst USSR Acad Sci) **13**:38–56

Castresana J (2000) Selection of conserved blocks from multiple alignments for their use in phylogenetic analysis. Mol Biol Evol **17**:540–552

Cavalier-Smith T (2014) Gregarine site-heterogeneous 18S rDNA trees, revision of gregarine higher classification, and the evolutionary diversification of Sporozoa. Europ J Protistol **50**:472–495

Cox FEG (1994) The evolutionary expansion of the Sporozoa. Int J Parasitol **24**:1301–1316

Desportes I, Schrével J (2013a) Treatise on Zoology—Anatomy, Taxonomy, Biology: Gregarines: Early Branching Apicomplexa **vol. 1**, Brill Publ., Leiden, Netherlands, 380 p

Desportes I, Schrével J (2013b) Treatise on Zoology—Anatomy, Taxonomy, Biology: Gregarines: Early Branching Apicomplexa **vol. 2**, Brill Publ., Leiden, Netherlands, 420 p

Edgar RC (2004) MUSCLE: multiple sequence alignment with high accuracy and high throughput. Nucleic Acid Res **35**:1792–1797

Grassé PP (1953)Grassé P-P (ed) Classe des grégarinomorphes (Gregarinomorpha, N. nov., Gregarinae Haeckel, 1866; gregarinidea Lankester, 1885; grégarines des auteurs). Traité de Zoologie. Masson, Paris, pp 590–690

Gunderson J, Small EB (1986) Selenidium vivax n. sp. (Protozoa, Apicomplexa) from the sipunculid *Phascolosoma agassizii* Keferstein, 1867. J Parasitol **72**:107–110

Hukui T (1939) On the gregarines from *Siphonosoma cumanense* (Keferstein). J Sci Hiroshima Univ **7**:1–23

Iritani D, Horiguchi T, Wakeman KC (2018) Molecular phylogenetic positions and ultrastructure of marine gregarines (Apicomplexa) *Cuspissella ishikariensis* n. gen., n. sp. and *Loxomorpha* cf. *harmothoe* from Western Pacific scaleworms (Polynoidae). J Eukaryot Microbiol **65**:637–647

Leander BS (2008) Marine gregarines – evolutionary prelude to the apicomplexan radiation? Trends Parasitol **24**:60–67

Levine ND (1971) Taxonomy of Archigregarinorida and Selenidiidae (Protozoa, Apicomplexa). J Protozool **18**:704–717

Levine ND (1976) Revision and checklist of the species of the aseptate gregarine genus *Lecudina*. Trans Am Microsc Soc **95**:695–702

Levine ND (1977a) Revision and checklist of the species (other than *'Lecudina*) of the aseptate gregarine family Lecudinidae. J Protozool **24**:41–52

Levine ND (1977b) Checklist of the species of the aseptate gregarine family Urosporidae. Int J Parasitol **7**:101–108

MacGregor HC, Thomasson PA (1965) The fine structure of two archigregarines, *Selenidium fallax* and *Ditrypanocystis cirratuli*. J Protozool **12**:438–443

Maddison WP, Maddison DR (2015) Version 3.04 Mesquite: a modular system for evolutionary analysis Version 3.04. http://mesquiteproject.org

Mathur V, Kolisko M, Hehenberger E, Irwin NAT, Leander BS, et al. (2019) Multiple independent origins of apicomplexan-like parasites. Curr Biol **29**:2939–2941.e5

Mellor JS, Stebbings H (1980) Microtubules and the propagation of bending waves by the archigregarine, *Selenidium fallax*. J Exp Biol **87**:149–161

Pasulka AL, Levin LA, Steele JA, Case DH, Landry MR, Orphan VJ (2016) Microbial eukaryotic distributions and diversity patterns in a deep-sea methane seep ecosystem. Environ Microbiol **18**:3022–3043

Paskerova G, Miroliubova T, Diakin A, Kováčiková M, Valigurová A, Guillou L, Aleoshin V, Simdyanov T (2018) Fine structure and molecular phylogenetic position of two marine gregarines, *Selenidium pygospionis* sp. n. and *S. pherusae* sp. n., with notes on the phylogeny of Archigregarinida (Apicomplexa). Protist **169**:826–852

Ronquist F, Huelsenbeck JP (2003) MrBayes 3: bayesian phylogenetic inference under mixed models. Bioinformatics **19**:1572–1574

Rueckert S, Horák A (2017) Archigregarines of the English Channel revisited: New molecular data on *Selenidium* species including early described and new species and the uncertainties of phylogenetic relationships. PLoS ONE **12(11)**: e0187430

Rueckert S, Leander BS (2008) Morphology and phylogenetic position of two novel marine gregarines (Apicomplexa, Eugregarinorida) from the intestines of North-eastern Pacific ascidians. Zool Scr **37**:637–645

Rueckert S, Leander BS (2009) Molecular phylogeny and surface morphology of marine archigregarines (Apicomplexa), *Selenidium* spp. , *Filipodium phascolosomae* n.sp., and *Platyproteum* n. gen. and comb. from North-Eastern pacific peanut worms (Sipuncula). J Eukaryot Microbiol **56**:428–439

Schrével J (1971a) Observations biologique et ultrastructurales sur les Selenidiidae et leurs conséquences sur la systématique des grégarinomorphes. J Protozool **18**:448–470

Schrével J (1971b) Contribution a l'étude des Selenidiidae parasites d'annélides polychètes. II. Ultrastructure de quelques trophozoïtes. J Protozool **7**:101–130

Schrével J, Valigurová A, Prensier G, Chambouvet A, Florent I, Guillou L (2016) Ultrastructure of *Selenidium pendula*, the type species of archigregarines, and phylogenetic position to other marine apicomplexans. Protist **167**:339–368

Simdyanov TG, Guillou L, Diakin AY, Mikhailov KV, Schrével J, Aleoshin VV (2017) A new view on the morphology and phylogeny of eugregarines suggested by the evidence from the gregarine *Ancora sagittata* (Leuckart, 1860) Labbé, 1899 (Apicomplexa: Eugregarinida). PeerJ **5**:e3354

Simdyanov TG, Kuvardina ON (2007) Fine structure and putative feeding mechanism of the archigregarine *Selenidium orientale* (Apicomplexa: Gregarinomorpha). Europ J Protistol **43**:17–25

Stebbings H, Boe GS, Garlick PR (1974) Microtubules and movement in the archigregarine, *Selenidium fallax*. Cell Tissue Res **148**:331–345

Stoeck T, Kasper J, Bunge J, Leslin C, Llyin V, Epstein S (2007) Protistan diversity in the Arctic: a case study of paleoclimate shaping modern biodiversity? PLoS ONE **2(8)**: e728

Talavera G, Castresana J (2007) Improvement of phylogenies after removing divergent and ambiguously aligned blocks from protein sequence alignments. Syst Biol **56**:564–577

Théodoridès J (1984) The phylogeny of the Gregarinia. Origins Life **13**:339–342

Tomova C, Geerts WJ, Muller-Reichert T, Entzeroth R, Humbel BM (2006) New comprehension of the apicoplast of *Sarcocystis* by transmission electron tomography. Biol Cell **98**:535–545

Trifinopoulos J, Nguyen LT, von Haeseler A, Minh BQ (2016) W-IQ-TREE: a fast online phylogenetic tool for maximum likelihood analysis. Nucleic Acids Res **44**:W232–W235

Wakeman KC, Heintzelman MB, Leander BS (2014) Comparative ultrastructure and molecular phylogeny of *Selenidium melongena* n. sp. and *S. terebellae* Ray 1930 demonstrate niche partitioning in marine gregarine parasites (Apicomplexa). Protist **165**:493–511

Wakeman KC, Leander BS (2012) Molecular phylogeny of pacific archigregarines (Apicomplexa), including descriptions of *Veloxidium leptosynaptae* n. gen., n. sp., from the sea cucumber *Leptosynapta clarki* (Echinodermata), and two new species of *Selenidium.* J Eukaryot Microbiol **59**:232–245